Disruptive effect of Dzyaloshinskii-Moriya interaction on the magnetic memory cell performance

J. Sampaio, A V Khvalkovskiy, M Kuteifan, M. Cubukcu, D Apalkov, V. Lomakin, V. Cros, N. Reyren

Disruptive effect of Dzyaloshinskii-Moriya interaction on the magnetic memory cell performance

J. Sampaio, A. V. Khvalkovskiy, M. Kuteifan, M. Cubukcu, D. Apalkov, V. Lomakin, V. Cros, and N. Reyren

Citation: Applied Physics Letters **108**, 112403 (2016); doi: 10.1063/1.4944419
View online: http://dx.doi.org/10.1063/1.4944419
View Table of Contents: http://scitation.aip.org/content/aip/journal/apl/108/11?ver=pdfcov
Published by the AIP Publishing

Disruptive effect of Dzyaloshinskii-Moriya interaction on the magnetic memory cell performance

J. Sampaio,[1,a)] A. V. Khvalkovskiy,[2,3] M. Kuteifan,[4] M. Cubukcu,[1] D. Apalkov,[2] V. Lomakin,[4] V. Cros,[1] and N. Reyren[1,b)]
[1]*Unité Mixte de Physique, CNRS, Thales, Univ. Paris-Sud, Université Paris-Saclay, 91767, Palaiseau, France*
[2]*Samsung Electronics, Semiconductor R&D Center (Grandis), San Jose, California 95134, USA*
[3]*Moscow Institute of Physics and Technology, State University, Moscow 141700, Russia*
[4]*Department of Electrical and Computer Engineering, University of California at San Diego, La Jolla, California 92093-0407, USA*

(Received 22 October 2015; accepted 5 March 2016; published online 16 March 2016)

In order to increase the thermal stability of a magnetic random access memory cell, materials with high spin-orbit interaction are often introduced in the storage layer. As a side effect, a strong Dzyaloshinskii-Moriya interaction (DMI) may arise in such systems. Here, we investigate the impact of DMI on the magnetic cell performance, using micromagnetic simulations. We find that DMI strongly promotes non-uniform magnetization states and non-uniform switching modes of the magnetic layer. It appears to be detrimental for both the thermal stability of the cell and its switching current, leading to considerable deterioration of the cell performance even for a moderate DMI amplitude.
[http://dx.doi.org/10.1063/1.4944419]

Recently, the development of magnetic random access memories (MRAM) for dense memory products such as dynamic or static random access memories became focused on magnetic cells with a high perpendicular magnetic anisotropy (PMA). These designs are believed to offer an improved thermal stability at very advanced technological nodes of 20 nm and below.[1,2] The PMA storage (a.k.a. "free") magnetic layer is based on magnetically soft CoFeB, which has a good lattice matching with the MgO barrier. The interface between MgO and CoFeB provides sufficiently strong PMA to hold perpendicular a CoFeB layer about 1 nm thick.[3] In order to further enhance the thermal stability of the cell, elements with a strong spin-orbit coupling (SOC), such as W, Pt, Ta, or Ir are often introduced into the free layer (FL).[4–7] However, recent studies demonstrated that a very large Dzyaloshinskii-Moriya exchange interaction (up to a large fraction of the Heisenberg exchange) may arise at the FM/SOC film interface.[8,9] Dzyaloshinskii-Moriya interaction (DMI) can dramatically change the magnetic state of the film. It was shown to induce a significant spin tilt at the borders,[10,11] for large DMI amplitude, it can stabilize cycloidal states and skyrmion lattices.[12] One might expect that the switching current could be reduced by the tilt produced even by the smallest DMI because the initial spin-transfer torque (STT) would be more efficient. Detailed simulations prove the situation to be more complicated. DMI also drastically changes the domain wall (DW) energy and, thus, the magnetic switching process,[13] both under field and under STT. Consequently, it can then be anticipated that DMI may affect the landscape of stable states and the reversal mechanisms, which are critical to the operation of MRAM cells. In this letter, we aim to analyze the influence of DMI on MRAM cells with perpendicular magnetization, in the range of DMI magnitude that may exist in typical material stacking used for MRAM elements.

DMI describes the chiral exchange interaction that favors rotations between neighboring spins.[14,15] The energy of an interfacial DMI between two neighboring spins S_1 and S_2 can be written as

$$E_{\mathrm{DM}} = \vec{d}_{12} \cdot (\vec{S}_1 \times \vec{S}_2), \tag{1}$$

where $\vec{d}_{12}$ is the DMI vector for these spins. For an interface between perfectly isotropic films, $\vec{d}_{12}$ is given by $d\,\hat{e}_z \times \vec{r}_{12}$, where d is the atomic DMI magnitude, $\hat{e}_z$ the unit vector normal to the interface, and $\vec{r}_{12}$ the unit vector pointing from S_1 to S_2. In the micromagnetic approximation of continuous magnetization, the interfacial DMI can be written as a volume energy density[10]

$$\mathcal{E}_{\mathrm{DM}} = D(m_z\,\partial_x m_x - m_x\,\partial_x m_z + m_z\,\partial_y m_y - m_y\,\partial_y m_z), \tag{2}$$

where $D = Cd/(at)$ is the micromagnetic DMI magnitude, C, a, and t are a geometric factor dependent on the film stacking, the lattice constant, and the thickness of the ferromagnetic film, respectively.

The DMI magnitude in thin magnetic films similar to those used in MRAM structures may reach up to a few mJ/m^2.[16,17] For example, recent measurements showed that $D = 0.053$ mJ/m^2 for Ta/CoFe 0.6 nm/MgO,[18] 1.2 mJ/m^2 for Pt/CoFe 0.6 nm/MgO,[18] and 7 mJ/m^2 for Ir/Fe monolayer.[8] As we show below, even for D in a range 0.3–1 mJ/m^2, we see a considerable impact on the MRAM cell performance. Performance of an STT-MRAM cell is characterized by two key parameters: the thermal stability factor Δ, and the critical switching current density j_{c0}.[2] Δ equals to the energy barrier height between the two magnetic states E_b normalized for the

a)Present address: Laboratoire de Physique des Solides, Univ. Paris-Sud, Université Paris-Saclay, CNRS, UMR 8502, 91405 Orsay Cedex, France.
b)Electronic mail: nicolas.reyren@thalesgroup.com

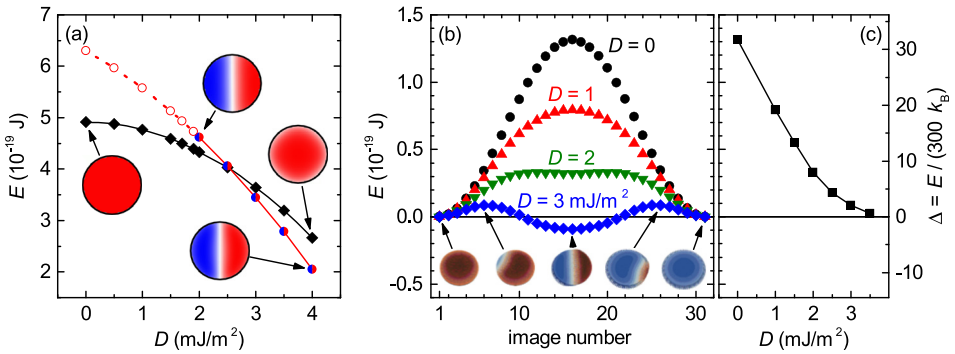

FIG. 1. Energy of static states in a nanodisk with DMI. (a) Energy of the quasi-uniform state (red line, circles) and of the DW state (black line, diamonds) versus DMI magnitude D, determined by micromagnetic simulations. The inset images show some of the stable and metastable configurations (where the colors red/white/blue correspond to the z magnetization component). The open/filled circles denote (meta) stable/unstable DW states. (b) Minimum energy paths of magnetic reversal for $D = 0$–3 mJ/m^2 calculated with NEB, showing the DW-mediated reversal. (c) Barrier height calculated from (b). The right axis shows the corresponding value of the room temperature thermal stability factor Δ.

operating temperature $\Delta = E_b/(k_BT)$, where k_B is the Boltzmann constant; it defines the information retention time as $t_0 \exp(\Delta)$, where t_0 is typically of the order of 1 ns. j_{c0} is the zero-temperature instability threshold current density, which defines the scale of the currents required for read and write operations. In our study, we investigate how Δ and j_{c0} change in presence of strong DMI effect using micromagnetic simulations. We exploit three numeric techniques: static and dynamic micromagnetic simulations using Mumax3[20] and OOMMF[19] (for preliminary studies at $T = 0$) open source codes, and nudged-elastic band (NEB) simulation of switching paths, using the FastMag code.[21] We use as a model system a perpendicularly magnetized disk of 32 nm diameter and 1 nm thickness, with the following material parameters: saturation magnetization (M_S) of 1.03 MA/m, exchange stiffness (A) of 10 pJ/m, perpendicular magnetocrystalline anisotropy (K_u) of 0.770 MJ/m^3, and a Gilbert damping factor (α) of 0.01. These parameters are typical of a perpendicularly magnetized CoFeB active layer in a magnetic tunnel junction (MTJ) used in an MRAM cell. With these values, we get an effective anisotropy for the disk $K_{\text{eff}} = K_u - \frac{1}{2}(N_z - N_x)\mu_0 M_s^2 = 187\,\text{kJ/m}^3$ (where N_i are the demagnetization factors of the disk[22]), corresponding to $\mu_0 H_{K_{\text{eff}}} = 364$ mT, a threshold DMI $D_c = 1.7$ mJ/m^2, and an $\Delta = K_{\text{eff}} V/(k_BT) = 36$, calculated in a uniform rotation approximation.

We first analyze how DMI affects the equilibrium quasi-uniform states. In these simulations made using the MuMax3 code (version 3.6.1), the magnetization was initially set up and let to completely relax. Once D increases, we see that DMI induces a radial tilt of the magnetization on the borders of the disk. As a result, the total micromagnetic energy (the sum of exchange, dipolar, anisotropy, and DMI energies) reduces with D (Fig. 1(a)). This observation is in agreement with other theoretical results reported for similar systems.[10,11]

Next, we study the evolution with D of the system energy once the magnetic disk has a straight DW in the middle, E_{DW}, see Fig. 1(a). In this simulation, the magnetization distribution was generated manually. (For metastable states, the system relaxes in the illustrated states, and the values for the unstable states were obtained using an ideal straight wall.) Even though this is not a true relaxed state, since it is symmetric it represents an energy extremum state on a possible switching path. We observe that the DMI lowers E_{DW} and stabilizes a Néel domain wall even if we started from a Bloch wall (for $D \geq 0.05$ mJ/m^2). The rate of variation of E_{DW} with D follows closely the theoretical value of $-\pi S$ ($= -10^{-16}$ J/(Jm^{-2})), where S is the DW surface.[11] For low D, the DW state has a higher energy than that of a uniform state and is unstable (open circles in Fig. 1(a)). But for $D > 1.8$ mJ/m^2, the DW state becomes meta-stable, which means that a DW may by trapped in the disk center if it gets there. For even larger D ($D > 2.6$ mJ/m^2), DW energy becomes lower than the energy of the uniform state; thus, it becomes the system ground state. This is an important result as this meta-stable DW state may force the use of higher writing currents, and impairs completely the required binary operation of a typical MRAM cell (as the system no longer has only two stable states).

From Fig. 1(a), we see that the energy difference between the uniform and DW state diminishes with D. To accurately estimate the dependence of the energy barrier on D, we exploit the NEB simulations[23,24] implemented in the FastMag code. NEB is a method to calculate a minimum energy path (MEP), i.e., the path in a configurational space connecting two ground states (up and down states for our disk) with a trajectory having minimum energy span. Using this method, it was shown recently that for PMA MRAM cells of sizes of even 20 nm or less, the domain-wall switching rather than the uniform rotation may be the primary thermal switching mechanism.[2]

In Fig. 1(b), we show the MEP calculated using the NEB method for D between 0 and 3.5 mJ/m^2, showing the intermediate magnetic states as insets. These simulations show that MEP is the DW-mediated reversal for all considered values of D (0–3.5 mJ/m^2), confirming the qualitative conclusion from Fig. 1(a). It also confirms existence of the metastable states for the DW for $D \gtrsim 2$ mJ/m^2 (corresponding to the appearance of an intermediate energy minimum in the curve of Fig. 1(b)). For larger D ($D > 2.5$ mJ/m^2), DW at the center of the disk becomes the ground state, and the highest energy point on MEP becomes an intermediate DW state close to an edge (see the magnetization distribution in the insets to Fig. 1(b)).

The energy barrier E_B and Δ as a function of D calculated by NEB simulations is plotted in Fig. 1(c). For $D = 0$

we get $\Delta = 33$, which is close to the analytical result $\Delta = 36$. This shows that without DMI, the energy difference between the uniform rotation and DW-mediated reversal is small, and DMI strongly promotes the DW-mediated reversal. Once D increases, Δ dramatically drops even for moderate values of D: by 20% to 27 with $D = 0.5$ mJ/m^2, and by 40% for $D = 1$ mJ/m^2, with a corresponding six orders of magnitude reduction of the retention time. For even larger D, we see that the barrier vanishes completely.

We now investigate the effects of DMI on the STT-induced switching performance. First, we simulate STT switching of our FL at zero temperature, assuming a perpendicular current uniformly distributed in the disk, with a spin polarization $P = 40\%$, producing an in-plane torque $\vec{m} \times \vec{p} \times \vec{m}$, $\vec{p}$ being the orientation of the injected spins (perpendicular to the plane), and no out-of-plane torque.[25,26] We considered square current pulses (instantaneous rise-time). The simulations show that the switching process starts by an excitation of oscillations that increase in amplitude, until magnetization breaks into the two-domain state with a subsequent reversal of the disk by a DW propagation. For $D = 0$, the amplitude of the oscillations increases gradually and uniformly in the disk, while, for finite D, the oscillations are uneven in amplitude, and strongly localized at the border of the disk. This may make the reversal process quite sensitive on the border properties, such as its shape and roughness, but also on the spatial discretization of the simulation (see supplementary material[27]). To avoid the artefacts related to the boundary discretization, we used the FastMag code in these simulations; its finite element micromagnetic solver allows defining the simulated disk with a smooth border.

For each value of the current density j, we extract the switching time t_{sw} of our FL, defined as the time when the FL magnetization crosses the equatorial plane (plane $z = 0$). In Fig. 2(a), we show the simulation result for $1/t_{sw}$ as a function of j, for D ranging between 0 and 2 mJ/m^2. We find that the switching time at a given current density is always larger for larger D. For an MRAM cell, the FL switching time t_{sw} varies inversely with j as follows:[28]

$$t_{sw}^{-1} \propto j/j_{c0} - 1. \tag{3}$$

We use Eq. (3) to fit the switching data and extract j_{c0}. It appears that even for large D the data is reasonably linear in j, which allows us to fit this data using Eq. (3). The fit result, j_{c0}, is shown in as a function of D in the inset to Fig. 2. We observe that j_{c0} increases with D: moderate at first with 15% at $D = 0.5$ mJ/m^2, but at a striking pace for larger D, reaching 70% for $D = 1$ mJ/m^2 and 110% for $D = 1.5$ mJ/m^2. For even higher values of D (>2 mJ/m^2), the system reaches often metastable states (with a DW), which impedes the determination of switching times.

As we mentioned above, DMI promotes switching via very non-uniform modes. Consequently, the cell switching performance and it dependence on D may become sensitive to the shape of the sample. In order to verify this suggestion, we perform additional simulations of the STT switching of the cells with different shapes. We find that while for $D = 0$, j_{c0} does not depend much on the cell, for finite D this dependence is considerable. For instance, j_{c0} for 1 mJ/m^2 ranged from 3.3 up to 8.3 MA/cm^2. These findings support the importance of border resonant modes in the reversal process in the presence of DMI.[29] See supplementary material for more information about the study of the role of edges and the dynamics of the switching.[27]

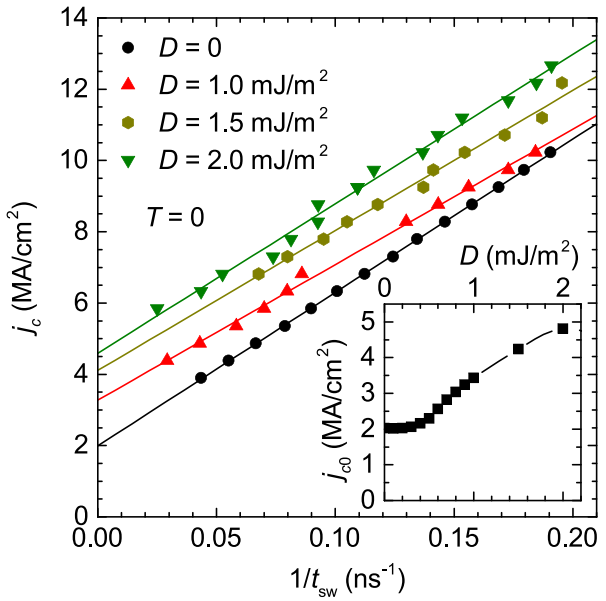

FIG. 2. Switching under current (STT) at zero temperature. Simulated applied current versus reciprocal switching time for different D values. The lines are linear fits to Eq. (3). The inset plot shows the extracted j_{c0} as a function of D.

We see that DMI leads to an increase in critical switching current (j_{c0}) with simultaneous decrease in the thermal stability factor (Δ). These opposing effects suggests that switching with STT at finite temperature might be very different from the $T = 0$ K case that we calculate in Fig. 2. To take the thermal effects and DMI into account in determining j_{c0}, we performed stochastic dynamical simulations, where we introduced a random magnetic field with a Gaussian amplitude distribution to simulate the effects of temperature.[20] We simulated repeatedly (at least twenty times) a current pulse with the same STT parameters as before for each set of parameters (D, j, and T), and calculated the mean switching time τ_{sw}. In the inset of Fig. 3, we show j versus $1/\tau_{sw}$ at $D = 1$ mJ/m^2 for various values of temperature. We extrapolated j_{c0} as before.

In Fig. 3, we show the variation of j_{c0} with D for various values of the temperature. We observe that j_{c0} always increases with D, with this increase being larger for higher T. The rise of j_{c0} is exacerbated by temperature: while at 0 K the j_{c0} at $D = 2$ mJ/m^2 is twice that of $D = 0$, at 300 K the difference is fivefold. For $D = 0$, we see that j_{c0} decreases for higher temperature. This result is in agreement with the stochastic macrospin simulations, which also show that even in a uniform switching mode and with a great statistical quality j_{c0} is expected to decrease with the temperature (see supplementary material for details[27]). However, for large D, we see that this dependence is reversed, and j_{c0} becomes larger for larger T.

Finally, the influence of DMI on both the MRAM switching current and thermal stability, quantified by j_{c0} and Δ, can also be seen in Figs. 3 and 1(c). We see readily that

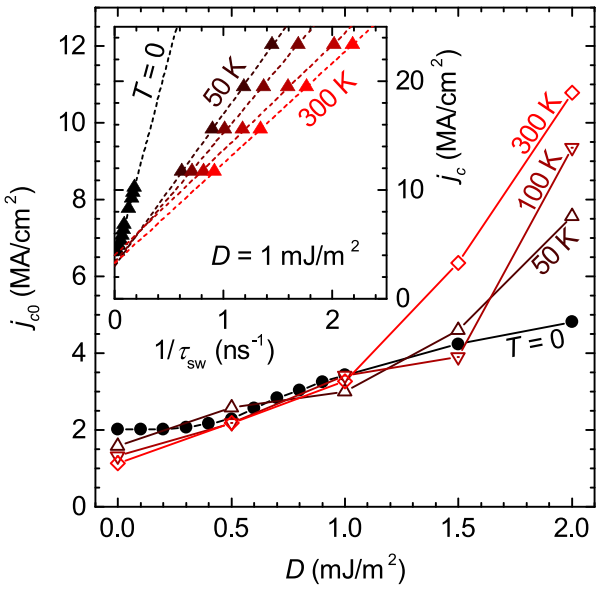

FIG. 3. Effects of DMI on the thermal stability and current induced switching of MRAMs. j_{c0} versus D for $T = 0$, 50, 100, and 300 K. The inset plot is the current versus the reciprocal mean switching time (τ_{sw}) for $D = 1$ mJ/m^2, for temperatures of 50, 100, 200, and 300 K, extracted from multiple (60 to 80) stochastic simulations; the data for $T = 0$ are also shown.

even a moderate DMI of $D \sim 0.5$ mJ/m^2 leads to an increase in j_{c0} and a large decrease in the thermal stability by tens of percent. This result emphasizes the importance of quantification and minimization of the DMI magnitude in materials used for the free layers in MRAM cells, possibly using materials that induce DMI of opposing sign.[30]

During the preparation of this article, an article by Jang *et al.* appeared,[31] which discusses some of the points also included here.

This work was supported by the Samsung Global MRAM Innovation Program, and by the NSF Grant Nos. DMR-1312750 and CCF-1117911.

[1]M. Gajek, J. J. Nowak, J. Z. Sun, P. L. Trouilloud, E. J. O'Sullivan, D. W. Abraham, M. C. Gaidis, G. Hu, S. Brown, Y. Zhu, R. P. Robertazzi, W. J. Gallagher, and D. C. Worledge, Appl. Phys. Lett. **100**, 132408 (2012).
[2]A. V. Khvalkovskiy, D. Apalkov, S. Watts, R. Chepulskii, R. S. Beach, A. Ong, X. Tang, W. H. Butler, P. B. Visscher, D. Lottis, E. Chen, V. Nikitin, and M. Krounbi, J. Phys. D: Appl. Phys. **46**, 074001 (2013).
[3]S. Ikeda, K. Miura, H. Yamamoto, K. Mizunuma, H. D. Gan, M. Endo, S. Kanai, J. Hayakawa, F. Matsukura, and H. Ohno, Nat. Mater. **9**, 721 (2010).
[4]K. Yakushiji, T. Saruya, H. Kubota, A. Fukushima, T. Nagahama, S. Yuasa, and K. Ando, Appl. Phys. Lett. **97**, 232508 (2010).
[5]H. Sato, M. Yamanouchi, S. Ikeda, S. Fukami, F. Matsukura, and H. Ohno, Appl. Phys. Lett. **101**, 022414 (2012).
[6]M. Yamanouchi, L. Chen, J. Kim, M. Hayashi, H. Sato, S. Fukami, S. Ikeda, F. Matsukura, and H. Ohno, Appl. Phys. Lett. **102**, 212408 (2013).
[7]S. Ishikawa, H. Sato, M. Yamanouchi, S. Ikeda, S. Fukami, F. Matsukura, and H. Ohno, J. Appl. Phys. **115**, 17C719 (2014).
[8]S. Heinze, K. Von Bergmann, M. Menzel, J. Brede, A. Kubetzka, R. Wiesendanger, G. Bihlmayer, and S. Blügel, Nat. Phys. **7**, 713 (2011).
[9]C. Moreau-Luchaire, C. Moutafis, N. Reyren, J. Sampaio, C. A. F. Vaz, N. Van Horne, K. Bouzehouane, K. Garcia, C. Deranlot, P. Warnicke, P. Wohlhüter, J.-M. George, M. Weigand, J. Raabe, V. Cros, and A. Fert, "Additive interfacial chiral interaction in multilayers for stabilization of small individual skyrmions at room temperature," Nat. Nanotechnol. (published online).
[10]J. Sampaio, V. Cros, S. Rohart, A. Thiaville, and A. Fert, Nat. Nanotechnol. **8**, 839 (2013).
[11]S. Rohart and A. Thiaville, Phys. Rev. B **88**, 184422 (2013).
[12]N. Nagaosa and Y. Tokura, Nat. Nanotechnol. **8**, 899 (2013).
[13]S. Pizzini, J. Vogel, S. Rohart, E. Jué, O. Boulle, I. M. Miron, C. K. Safeer, S. Auffret, G. Gaudin, and A. Thiaville, Phys. Rev. Lett. **113**, 047203 (2014).
[14]I. Dzyaloshinsky, J. Phys. Chem. Solids **4**, 241 (1958).
[15]T. Moriya, Phys. Rev. **120**, 91 (1956).
[16]J. H. Franken, M. Herps, H. J. M. Swagten, and B. Koopmans, Sci. Rep. **4**, 5248 (2014).
[17]K.-S. Ryu, S.-H. Yang, L. Thomas, and S. S. P. Parkin, Nat. Commun. **5**, 3910 (2014).
[18]S. Emori, E. Martinez, K.-J. Lee, H.-W. Lee, U. Bauer, S.-m. Ahn, P. Agrawal, D. C. Bono, and G. S. D. Beach, Phys. Phys. B **90**, 184427 (2014).
[19]M. J. Donahue and G. Porter, *OOMMF User's Guide, Version 1.0* (NIST, 1999).
[20]A. Vansteenkiste, J. Leliaert, M. Dvornik, M. Helsen, F. Garcia-Sanchez, and B. Van Waeyenberge, AIP Adv. **4**, 107133 (2014).
[21]R. Chang, S. Li, M. V. Lubarda, B. Livshitz, and V. Lomakin, J. Appl. Phys. **109**, 07D358 (2011).
[22]D. X. Chen, J. A. Brug, and R. B. Goldfarb, IEEE Trans. Magn. **27**, 3601 (1991).
[23]R. Dittrich, T. Schrefl, D. Suess, W. Scholz, H. Forster, and J. Fidler, J. Magn. Magn. Mater. **250**, 12 (2002).
[24]I. Tudosa, M. V. Lubarda, K. T. Chan, M. A. Escobar, V. Lomakin, and E. E. Fullerton, Appl. Phys. Lett. **100**, 102401 (2012).
[25]C. Slonczewski, J. Magn. Magn. Mater. **159**, L1 (1996).
[26]L. Berger, Phys. Rev. B **54**, 9353 (1996).
[27]See supplementary material at http://dx.doi.org/10.1063/1.4944419 for details about the effects related to edge roughness, the intermediate states and the temperature dependence of j_{c0}.
[28]J. Z. Sun, Phys. Rev. B **62**, 570 (2000).
[29]J.-V. Kim, F. Garcia-Sanchez, C. Moreau-Luchaire, V. Cros, and A. Fert, Phys. Rev. B **90**, 064410 (2014).
[30]A. Hrabec, N. A. Porter, A. Wells, M. J. Benitez, G. Burnell, S. McVitie, D. McGrouther, T. A. Moore, and C. H. Marrows, Phys. Rev. B **90**, 020402 (2014).
[31]P.-H. Jang, K. Song, S.-J. Lee, S.-W. Lee, and S.-W. Lee, Appl. Phys. Lett. **107**, 202401 (2015).